Bulletin of the Mineral Research and Exploration

http://bulletin.mta.gov.tr

SEDIMENTOLOGY, MINERALOGY AND ORIGIN OF THE FIRST DISCOVER MAGNESITE-DOLOMITE BELT IN MA'RIB DISTRICT, SW ARABIAN PENINSULA

Sa'ad Zeki A.kader AL-MASHAIKIE[a]

[a]Dept. of Earth Sciences, Collage of Sciences, University of Baghdad, Al-Jadriyah, Baghdad, IRAQ

Research Article

ABSTRACT

Magnesite mineralization of high purity was discovered and described herein for the first time from metamorphosed folded belt from Al-Thanyiah locality in Rub'Al-Khali sector, 360 km east of Sana'a City, northwest Yemen. The magnesite-metamorphic belt, belonging to the Precambrian/Neoproterozoic age? comprises thrust belt, which trends generally N-S direction. Magnesite mineralization was identified in an extended carbonate-metamorphic belt for several tens of kilometers cf. 31 km and occurred in association with 8 stratigraphic units. The thicknesses of pure magnesite bearing units are variable and ranges from 20 to 60 m, associated with dark green chlorite-schist with intersecting huge ultrabasic intrusions. Geochemical, mineralogical and petrographic analyses show that the magnesite concentrations in the stratigraphic units are ranging from 78% up to high purity of 99.6% cf. 35 to 48.9% MgO, with minor dolomite and calcite respectively. Little to rare content of talc and brucite were also recognized. Two thick, productive and high purity magnesite beds, the first is of 40 m thick and the second is 60 m in thickness, which reveals more than 95% $MgCO_3$ and considered to be economic. The suggested origin of the magnesite mineralization is coming from high stress of regional metamorphism associated with ultramafic *intrusions* cf. amphibolite and harzburgite associated with diagenetic solutions rich in Mg^{2+}, associated with the heat of magma. The alteration of dolomite to magnesite was formed by multiple phases to transform calcite and/or dolomite to magnesite.

1. Introduction

Magnesite beds in Al-Thanyiah metamorphic belt are unusual formations in the Arabian Peninsula. The magnesite beds are very thick and of high purity in composition. The belt is lying 360 km east of Sana'a Capital City and 130 km from Ma'rib city. It is extended for more than 31 km in a belt, which is formed by metamorphosed carbonates interbedded with thick green schist beds (Al-Mashaikie, 2006) (Figure 1 and 2).

It is not well understood how the Mg-rich carbonates of Al-Thanyiah area formed and they have attracted the attention of the author because: i) they are among the oldest carbonates preserved in the southern Arabian Peninsula as well as in Yemen, ii) they contain more than one magnesite bearing thick horizons (Al-Mashaikie, 2006, 2007, 2008) and, iii) they record a complex diagenetic history, which may be useful in understanding the mechanisms that resulted in the formation of similar deposits elsewhere in the world.

Magnesite precipitates in the modern coastal and continental environments (Pueyo and Inglés, 1987; Schroll, 2002) as well as in ancient sedimentary sequences (Zachmann, 1989). The formation of magnesite in sedimentary conditions is always considered to be secondary and as a typical product of advanced diagenesis (Müller et al., 1972; Tucker and Wright, 1990). Pohl (1990) distinguished two types of economically important magnesite deposits: 1) cryptocrystalline magnesite with Mg sourced by ultramafic magmatic host rocks (Pohl, 1989), and 2) stratabound lenses of coarse crystalline magnesite, which are associated with marine platform environments such as those examined in this paper.

The magnesite deposits are present as extended thick beds in Al-Thanyiah area without any lens like strata. The magnesite beds are interbedded with dolomite beds as well as thick green schist horizons.

The origin of the second type of magnesite is controversial and there are two main models postulated for its formation. In the first model, magnesite
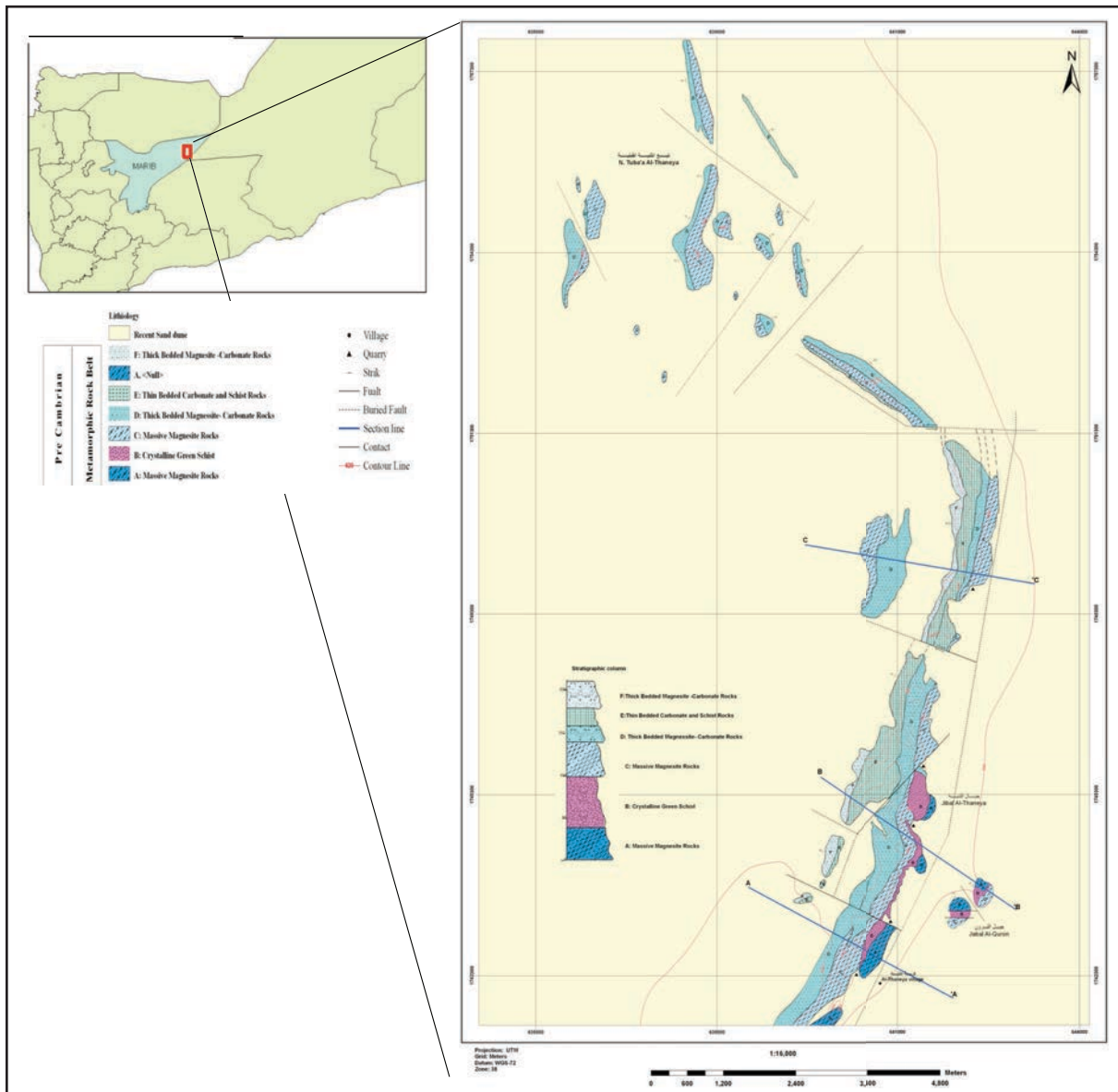

Figure 1- The geological map of the Al-Thanyiah Belt shows the stratigraphic units of the major belt (the map constructed by the author Al-Mashaikie (2006)).

is considered to be a product of synsedimentary processes related to evaporitic conditions or to early diagenetic transformations of carbonates (Pohl, 1990; Tucker and Wright, 1990; Melezhik et al., 2001). Magnesite precipitation has been suggested to occur in evaporitic sabkha-type environments (Quemeneur, 1974) or from Mg-concentrated brines originated by early diagenetic compaction of clays (Siegl, 1984).

The second model considers an epigenetic origin, which involves hydrothermal/ metasomatic replacement of dolostones during thermal events (Tucker, 1982; Dulski and Morteany, 1989; Zachmann

and Johannes, 1989; Lugli et al., 2000; Machel and Lonnee, 2002; Kilias et al., 2006).

Al-Mashaikie (2006) was discovered and recorded the magnesite rocks belt first time ever. The chemical analysis of collected rock samples show that the percentages of magnesite in these rocks range from 78.22% up to 97.78% with MgO percentages vary from 35.22% up to 47.65%.

Geomine Company (1984-1985) was working in the areas in NW Yemen in the proximity of border of Yemen Arab Republic with Saudi Arabia. They
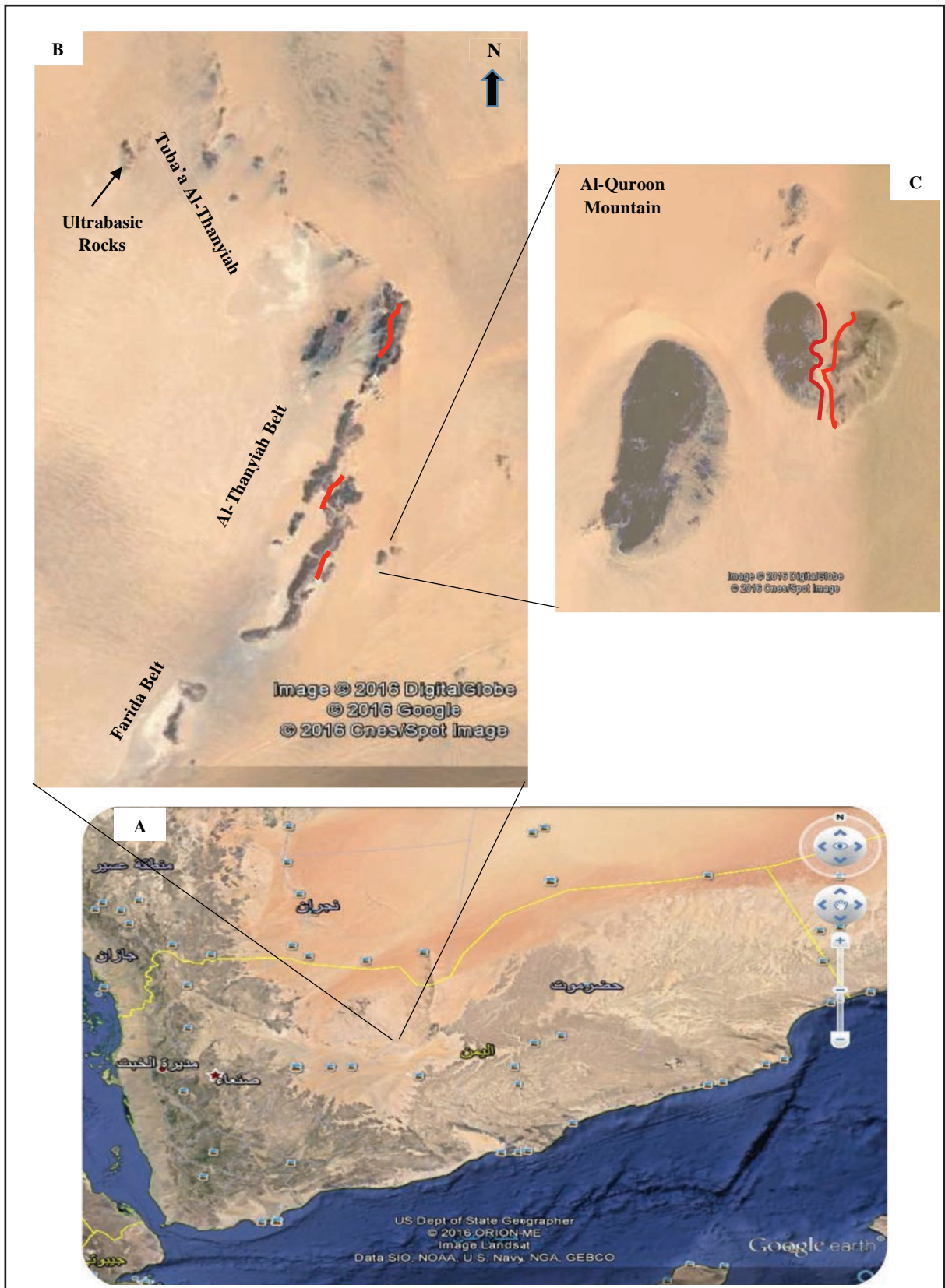
Figure 2- Satellite images show (A) general map of Yemen, (B) The Al-Thanyiah Belt with subdivisions of Fariedah, AL-Thanyiah and Tuba'a
Al-Thanyiah belts with the ultrabasic intrusion (the red lines, and (C) Al-Quroon Mountain show large ultrabasic intrusion in between
the red lines.

reported several hills amounting about 12 km length and a part as 300m width, and 25-50 m height trending north – south and dip 60-70 ^{0} to the west. They are consisted of marbles (crystalline limestone, dolomitic limestone and dolomites) of various colors including white–gray, gray–yellowish, black–colored with intermediate hues. The rocks have crystalline, granular and granoblastic structures, compact texture, sometimes with vacuoles and irregular breaks (Geomine Company, 1984-1985). Beydoun et al. (1998) referred to rock successions in Al-Thanyiah area as unknown rock units of Cambrian age.

In this paper, we discuss the origin of the magnesite and dolostone of the Neoproterozoic (Ediacaran?) deposits of the Al-Thanyiah metamorphosed belt (Al-Mashaikie, 2006). Sedimentology, petrology, diagenesis and geochemical analyses permit to establish a dataset that characterize magnesite deposits formed under hydrothermal conditions. This model is useful to understand the genesis of similar magnesian deposits in other parts of the world and offers an alternative explanation for magnesite deposits that have been interpreted as products of evaporation processes.

2. Geological Setting

The Neoproterozoic (?) bed rocks are crop out in the Rub'Al-Khali Sector of Northwest Yemen. This area is characterized by extensive exposure of high grade metamorphosed sedimentary series of the Ediacaran (?) schist-greywacke-carbonate complex. Al-Thanyiah Belt surrounded by recent sand dunes of the Rub'Al-Khali Desert (Figure 1 and 2).

The Metamorphic Belt is composed of interbedded thick horizons of magnesite, magnesite/dolomite, dolomite, and green schist (Figure 3). These successions are most probably deposited on a mixed carbonate–siliciclastic platform. These rocks are exposed in an over-thrust fold intersected with several reverse faults. These rocks are not described or recorded previously, and the age is still unknown. The main thrust belt trends almost N-S direction. The geological age suggested herein is according to the stratigraphic correlation with the Oman and Ethiopia (Brasier et al., 2011).

The Neoproterozoic (?) carbonate platform was never reported previously in Yemen. Only a preliminary report was written after detailed field work and lab analyses for the collected samples (Al-Mashaikie, 2006).

The major belt of Al-Thanyiah outcrops is intersected by major thrust fault forming overturned fold e.g. both structures trend N-S direction. The upthrow part represents the out crop successions e.g. the western part of the mountain, while the eastern down throw part is sinking under the recent sand dunes (Figure 1). All these features are the result of complex tectonic evolution. These magnesite-carbonate metamorphic belt is cut by huge ultrabasic intrusions.

The area is subjected to intense regional metamorphism as the major tectonic event that affected the Precambrian basement rocks in Yemen (Beydoun et al., 1998). This magnesite-carbonate metamorphic belt most probably represents cap carbonate rocks that followed the Ediacaran main glacial period in Yemen.

3. Methodology

Conventional petrography analyses were performed on selected 50 thin sections cut perpendicular to the bedding plane to present all mineralogical constituent and variations in the rock sample, following the procedure listed in Tucker (1988). Polarizing microscope type Leitz-LABOURLUX 12 Pol was used for the petrographic examinations.

Powdered samples (18) were mineralogically examined using Philips PW-1710 X-ray diffraction (XRD) system operating at 40 kV and 40 mA, and employing mono-chromated CuKα radiation. The XRD spectra obtained from 2 to 66° 2θ. XRD analysis were carried out in the labs of Natural Resources Authority, Amman-Jordan.

Moreover, geochemical analysis were carried out to determine the MgO% and CaO% contents to determine the magnesite concentration in the rocks. The X-ray fluorescence technique was employed a Bruker Tiger S-6 XRF instrument to analyze 23 samples for their major element contents. Both XRD and XRF analyses were carried out in the labs of the Natural Resources Authority in the Hashemite Kingdom of Jordan and labs of University of Beijing in China.
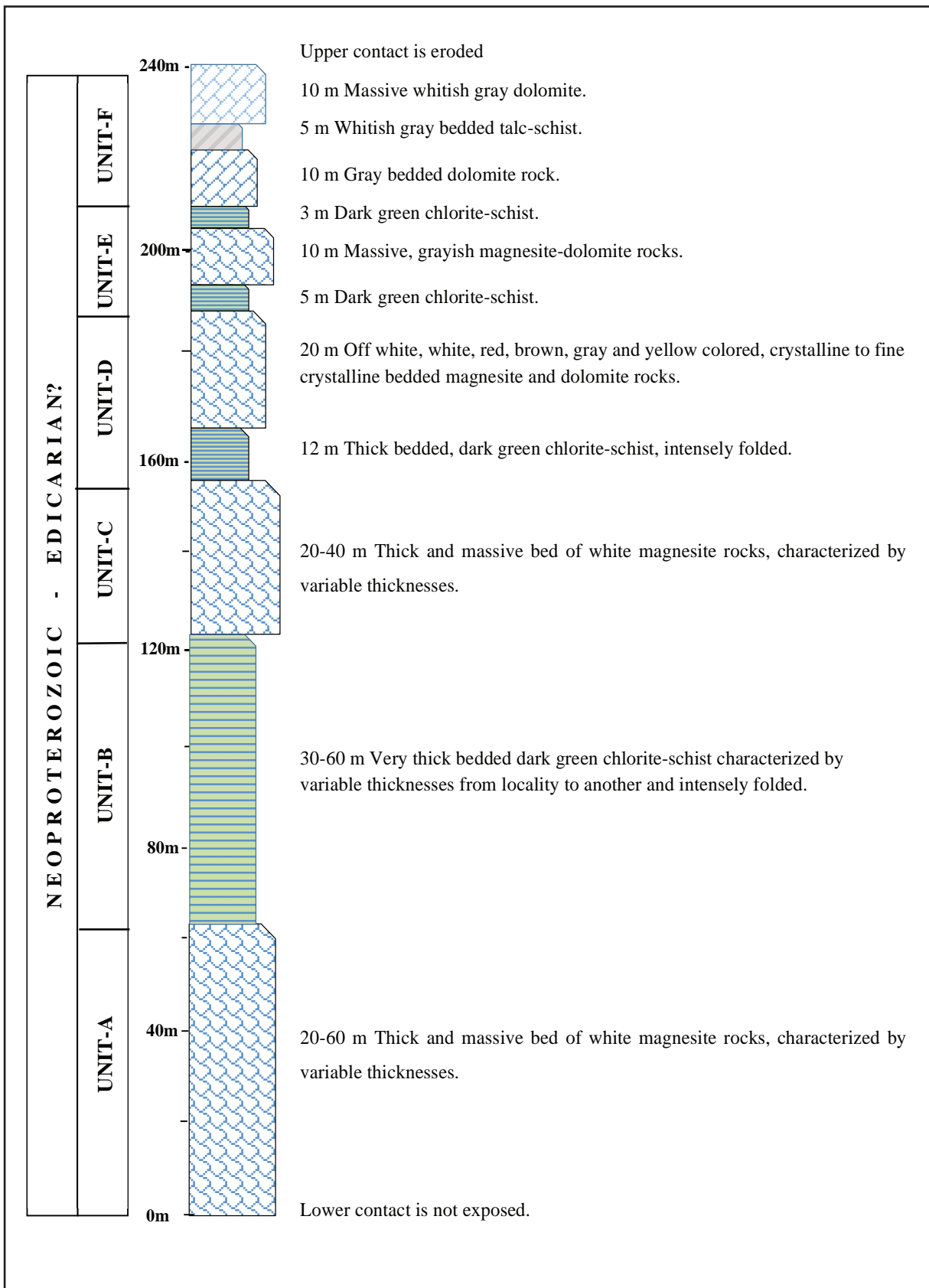
Figure 3- Stratigraphic section of the Al-Thanyiah Belt Rocks presents different stratigraphic units of magnesite, dolomite, chlorite-schist and talc-schist, which are cropping out in the studied area.

4. Field Characteristics of Magnesite Belt

Detailed and comprehensive field works were carried out to examine and define Al-Thanyiah magnesite belt:

Stratigraphic Name: Al-Thanyiah Group is suggested as a new name for this new stratigraphic unit to introduce in the geological column of Yemen, where there is no previous record for it.

Geologic Age: The previous works was not defining the age of Al-Thanyiah belt. Field observations suggest that these rocks are of Neoproterozoic-Ediacaran age, in which the rock successions are underlain by glaciogenic rocks. Moreover, the rocks are intensely tectonized where any fossils were observed.

Morphotectonic: Al-Thanyiah region comprises a carbonate-metamorphic major belt trends generally N-S and surrounded by recent sand dunes. The major belt composed essentially of three belts e.g. southern Fariedah, middle Al-Thanyiah and north Tuba'a Al-Thanyiah. These belts are separated by strike-slip faults, which tends to tilt the south Fariedah toward SE and the Tuba'a Al-Thanyiah toward NW (Figure 2). Two major tectonic events are reported in the Al-Thanyiah belt, overturned fold and the thrusting reverse fault (both are dipping more than 120^0). The thrusting reverse fault is intersected the Fariedah and Al-Thanyiah belts along the fold axis and from the eastern side, while the Tuba'a Al-Thanyiah is intersected along the fold axis and from the western side. Several minor normal and over-thrust faults are intersected the bed rocks. The morphotectonic represented by series of low elevation mountains standing up sand dunes of the Yemeni side of the Rub'Al-Khali Desert.

The width of the Al-Thanyiah belt ranges from 0.5 to 1.35 km and extended for more than 31 km the general height ranges from 90 to 135 m above the land surface and the whole area is elevated for 800-900 m above sea level (a.s.l.).

The south Fariedah is extended for about 3 km, middle Al-Thanyiah belt is 17 km and Tuba'a Al-Thanyiah for about 11 km. The geology of the belt reflects some complications due to intense tectonism. According to intense thrusting the eastern limb of Al-Thanyiah major fold was subducted under the sand dunes.

Thickness: The thickness of the whole successions reaches more than 240 m including green schist beds. The magnesite-bearing units attain a part as 15 m up to 60 m thick, while the schist beds are ranging from 6 m up to 70 m in thickness. The intersecting ultra-basic rocks range from 10 m up to 50 m thick.

Boundaries: The upper surface of the carbonate rocks was eroded and sometimes not exposed and the bottom are buried under the sand dunes of the desert.

Sedimentology: The magnesite and dolomite rocks examined here appear in six distinct units at the Al-Thanyiah area. The lower Unit-A was studied in the three main belts of Fariedah, Al-Thanyiah and Tuba'a Al-Thanyiah, sections (Plate I). Carbonate units (magnesite and dolomite rocks) are about 240 m thick and are separated by intercalations of metamorphosed thick and thin siliciclastic beds of most probably sandstones and shales (Plate I, photo 3,6,7, plate II, photo 5,6). The rocks are mostly crystalline, and in places the magnesite crystals reach about 0.1 to 0.3 m in size (Plate II, photo 1).

The successions of the rocks are composed of magnesite, magnesite-dolomite, chlorite-schist, talc-schist, talc, and ultra-basic rocks. These rocks are developed in the areas of the Precambrian basement rocks e.g. granite, schist, talc, ultra-basic igneous rocks, and amphibolite overlies with magnesite-dolomite successions. The basement rocks are intensely tectonized. In the field, the magnesite rocks are white, off-white, gray, red, yellow and black in color with intermixing of white and pink colors. While the dolomite rocks are mostly of gray color.

The six magnesite-carbonate units show similar features although most of their primary structures and textures have been erased by magnesitization and dolomitization processes.

i) Magnesite rocks appear as massive and bedded and sometimes laminated. The massive beds are very thick and attain more than 20 m in thickness (Plate I, photo 2,3,6). These beds consist of coarse mosaic magnesite crystals with little brucite, and talc crystals (Plate III, photo 1-4). Another identified magnesite rocks appears as thin beds. These beds exhibit porphyritic texture represented by coarse crystals surrounded with small crystal (Plate III, photo 5).

ii) Dolomites appear as both massive and thinly bedded/laminated beds. Massive dolomites occur in beds ranging from 0.5 to 2 m in thickness (Plate I, photo 6, Plate II, photo 7). These beds consist of coarse mosaic dolomite including ghosts of dark cloudy twining laminae. In addition, there are undulated laminations that is thought as stromatolite laminations (Dragastan and Richter, 2011; Perri et al., 2012) also confirming the shallow nature of the depositional environment.

iii) Intensely metamorphosed siliciclastic deposits formed by thin (mm-cm) alternations of sandstones and shales (Plate I, photo 3,6). These rocks comprise chlorite-schist and talc-schist, dark green, black, and grayish white in color. The architectural facies arrangement is that characteristic of a mixed carbonate–siliciclastic platform environment, which has been developed during Ediacaran (?) time (IUGS, 2009). The suggested depositional environment was characterized by carbonate deposits that would represent the shallower inter to supratidal facies, whereas the clastic deposits correspond to deeper and higher energy environments (subtidal).

5. Petrography

The magnesites and dolomites of the Al-Thanyiah Group comprises magnesite-carbonate successions intercalated with metamorphosed siliciclastic deposits. The most extensive cases are the formation of magnesite, which shows different textures. In all of Al-Thanyiah three belts, magnesitization advanced through fractures, faulting, cavities, and bedding planes; it was pervasive and totally replaced the dolomitic rocks.

The Al-Thanyiah Belt is intersected with several dikes and intrusive bodies of ultrabasic igneous rocks of peridotite and hornblendite compositions. The peridotite rocks composed of majority olivine and pyroxene with minor anorthite, while the hornblendite is composed totally of hornblende mineral.

In the studied sections of southern Farieda, middle Al-Thanyiah and northern Tuba'a Al-Thanyiah belts (Plate I, photo 1-5), replacement mostly advanced totally for the magnesite-productive beds. The main dominant mineral is magnesite with minor dolomite, calcite, talc, brucite and rarely forsterite.

Magnesite

Magnesite was identified as four different diagenetic textural phases termed M1, M2, M3 and M4.

1. Magnesite 1 (M1) is composed of unimodal, euhedral, planar boundary and mosaic very coarse crystals with strong undulatory extinction. Crystal size ranges from mm to several centimeters. M1 is free of Fe-minerals (Plate III, photo 2) and associated with minor talc and brucite minerals. No relics exist of the previous texture of the rock. This magnesite initially occurs along cavities, fracture and fault planes (Plate II, photo 1,5,6,8), and ultimately totally replace the previous dolomite rocks to form a massive beds of magnesite.

2. Magnesite 2 (M2) is composed of bimodal, subhedral, planar and irregular boundary crystals with strong undulatory extinction. Crystal size ranges from mm to several centimeters. M2 is also free of Fe compounds (Plate III, photo 3) and associated with minor talc and brucite minerals. No relics exist of the previous texture of the rock. This magnesite initially occurs along cavities, fracture and fault planes and ultimately totally replace the previous dolomite rocks to form a massive beds of magnesite.

3. Magnesite 3 (M3) is composed of unimodal, anhedral, non-planar boundary crystals with undulatory extinction. Crystal size ranges from mm to several centimeters. M3 is free of Fe-minerals crystals (Plate III, photo 4) and associated with minor talc and brucite minerals. No relics exist of the previous texture of the rock. This magnesite initially occurs along cavities, fracture and fault planes and ultimately completely replace the previous dolomite rocks to form a massive beds of magnesite.

4. Magnesite 4 (M4) is composed of porphyritic bimodal, subhedral planar to non-planar boundary crystals with undulatory extinction. M4 is totally free of Fe-minerals (Plate III, photo 5) and associated with minor dolomite, talc and brucite minerals. No relics exist of the previous texture of the rock. This magnesite initially occurs along cavities, fracture and

fault planes and ultimately totally replace the previous dolomite rocks to form a massive beds of magnesite.

Dolomite: Two different dolomite textures were identified (D1 and D2):

1. Dolomite 1 (D1) is characterized by non-planar, anhedral closely packed with subhedral crystals (0.01 to 0.3 mm) with undulatory extinction (Plate III, photo 5). The dolomite crystals are with cloudy shades.

2. Dolomite 2 (D2) consists of mosaic of coarser, 0.1 to 1 mm size crystals. Most crystals are clear and mostly have planar and non-planar crystal boundaries. The crystals are characterized by bands of cloudy shades (Plate III, photo 6). D1 and D2 textures are of low percentages in the magnesite-productive units. This is identified from the petrographic examination and confirmed by the XRD and XRF analyses.

Talc: Talc appears as scattered euhedral to subhedral laths and was recognized in all of the studied beds. Talc is commonly associated with coarse magnesite crystals along fractures or between the boundaries of the crystals. It is almost lath like shape and sometimes present as aggregates (Plate III, photo 5,6).

Brucite: Brucite is recognized in all of the studied rock samples and associated with magnesite mineral. It was identified as single crystal appears in the boundaries between magnesite and dolomite crystals, and along the fractures and micro-fault planes. It attains prismatic or irregular crystal shapes (Plate III, photo 3).

Other diagenetic minerals: Calcite was identified as fine crystals and rare to minor mineral in some of the studied samples. It is most probably of late diagenetic origin. Moreover, some clay minerals cf. montmorillonite, were identified due to diagenetic alteration of talc and brucite minerals.

6. Mineralogy

The XRD analyses were performed for selected samples collected from different localities across the Al-Thanyiah Belt. The results showed that the majority of the samples are magnesite with minor dolomite, talc, brucite, calcite, and sometimes montmorillonite clays (Table 1 and 2, Figure 4). Table 2 shows that 5 samples comprise magnesite productive horizons, which are composed of MgO % from 75 to 95%. The other samples are dolomitic magnesite, dolomites and two samples are marble rocks

7. Geochemistry

Geochemical analyses were carried out using XRF technique to define and confirm the presence of magnesite deposits and to differentiate the associated dolomite and calcite minerals and rocks. The results of XRF analyses are listed in table 3. These results are coincided with the XRD analyses.

Element composition: Average composition of the major oxides in the studied samples is listed in table 3. The XRF analyses reveal four productive units containing magnesite with high MgO wt. % concentrations. The MgO concentrations in these beds range from 43.69 % up to 45.6 %, while the CaO

Table 1- The XRD results of selected rock samples from Al-Thanyiah region shows the relative abundance of the mineralogical constituents of essential magnesite, calcite and dolomite minerals with minor talc, brucite and quartz (Labs of Authority of natural resources Amman-JORDAN).

Sample no	Calcite	Quartz	Muscovite	Dolomite	Magnesite	Smectite	Brucite	Talc	Kaolinite	Ilmenite
S-1	*	-	-	*	***	*	-	*	-	-
N-3	***	**	*	-	-	*	-	-	-	*
N-4/3	-	-	-	***	-	*	*	-	-	-
N-5	*	-	-	***	***	*	*	-	-	-
N-8	-	-	-	***	-	*	*	*	*	-
N-7	-	***	-	***	*	-	-	*	-	-
N-2	-	***	-	***	-	*	*	-	-	-
N-7/2	-	-	-	***	*	*	*	*	-	-
N-4	*	-	-	*	***	*	*	*	-	-
G-M	***	*	*	**	-	*	*	-	-	-

Major ***   Minor **   Trace *

Note: All of the samples are form carbonate rocks e.g. magnesite, dolo-magnesite, dolomite and marble (calcite).

Table 2-   XRD results of selected rock samples from Al-Thanyiah region shows the mineralogical constituents includes essential magnesite, dolomite and calcite minerals with minor talc, brucite and quartz (Analysis was carried out in the University of Beijing-CHINA).

Örnek no.	Mineralogical constituent %											
	Manyezit	Dolomit	Kalsit	Talk	Brusit	Q	Feldspat	Mika-Muskovit	Serpantin	Periklas	Klorit	Toplam
N4-L1	95	1		4	1							100
N5	94			6								100
N6-L1	85	1		13		1						100
N7-L1	86			14								100
N3-L1		98		2								100
N8-L1	75	22		3								100
N9-L2	68	28		4								100
R1-3	60	32		8								100
R1-2	51	42		6	1							100
R2-2	39	52		8	1							100
R2-4	1	94		5								100
N4-L3	2	94			1				3			100
N10-L1		98					2					100
N6-L2		83	1	16								100
N7-L3		82	1				13				4	100
N2-L1	8	73		14		5						100
N10-L2			98			2						100
N10-L4			67			23		10				100

R=Fariedah Belt   N 1-8 =Al-Thanyiah Belt   N10 = Tuba'a Al-Thanyiah samples
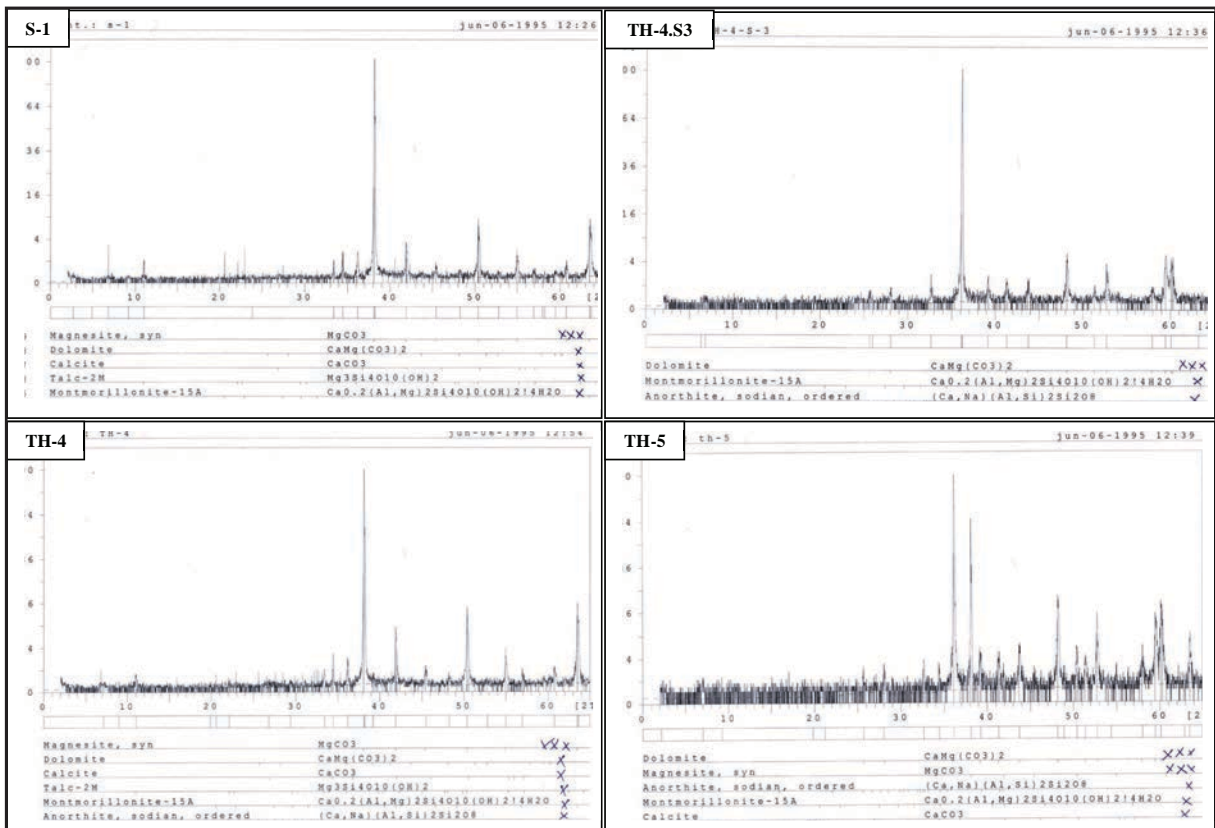
Figure 4- XR-Diffractograms of selected sample shows the majority of magnesite mineral in the productive beds with minor dolomite and rare calcite and talc minerals.

concentrations in the same beds are 0.09 % to 0.54 % respectively. Otherwise, the XRF analyses show six beds composed of almost pure dolomites, with two marble beds composed of pure calcite.

Three of magnesite phases are similar M1, M2 and M3 e.g. N4-L1, N5, N6-L1, while N7-L1 is differ in MgO% (45.6, 45.39, 43.76wt. %), FeO (0.37, 0.38, 0.3wt. %), and MnO % (0.007, 0.002, 0.012), respectively, while M4 e.g. N7-L1 has MgO % (43.69), FeO % (0.19) and MnO % (0.014).

8. Discussion

The critical examination of the different textures observed in the outcrop and thin section studies and their relationships, along with the geochemical characteristics permit to establish the sequence of diagenetic events that lead to the formation of the phases previously described (Figure 5).

A. First Dolomitization Event: The pre-existing limestones which was deposited in a mixed siliciclastic–carbonate platform is undergone intense dolomitization (Figure 5). Dolomitization processes only partially preserved the original depositional texture of the priory limestone. D1 and D2 are the result of replacement processes via the circulation of Mg^{2+} rich solutions, most probably created by progressive evaporation of marine waters within the peritidal environment (sabkha dolomitization model) (Morse and MacKenzie, 1990). Moreover, during the field works, the stromatolite algae were preserved in some examined beds, which refers to the formation of synsedimentary dolomites in the presences of microbial math cf. microbialites, in shallow marine setting (Prasannakumar et al., 2002; Teedumäe et al., 2006; Wacey et al., 2007; Spadafora et al., 2010; Herrero et al., 2011; Nash et al., 2011; Meister et al., 2013). The textural and geochemical evidences do not evoke a clear dolomitization mechanism due to intense tectonism and the rocks components

Table 3- XRF-Geochemical analysis results of selected samples from Al-Thanyiah region (Analysis was carried out in the University of Beijing-CHINA).

Sample no.	Major oxides %											
	Al2O3	CaO	MgO	Fe2O3	SiO2	MnO	Na2O	K2O	P2O5	TiO2	LOI	Total
N4-L1	0.34	0.54	45.6	0.37	3.21	0.007	0.22	0.01	0.005	0.014	49.55	99.86
N6-L1	0.28	1.34	43.76	0.3	5.98	0.012	0.18	0.01	0.016	0.013	47.99	99.88
N7-L1	0.28	0.09	43.69	0.19	4.84	0.014	1.94	0.01	0.003	0.014	48.74	99.81
N3-L1	0.39	30.51	19.27	0.2	2.8	0.038	0.65	0.01	0.011	0.01	46.02	99.91
N8-L1	0.28	9.28	38.09	0.39	3.38	0.001	0.01	0.01	0.005	0.015	48.43	99.88
N9-L2	0.22	16.96	30.73	0.28	4.25	0.002	0.91	0.01	0.001	0.013	46.48	99.86
R1-3	0.45	15.83	31.77	0.17	5.33	0.001	0.19	0.01	0.003	0.014	46.12	99.87
R1-2	0.28	20.88	27.86	0.32	4.71	0.002	0.5	0.01	0.005	0.014	45.3	99.87
R2-2	0.32	21.11	27.44	0.31	3.67	0.003	0.76	0.01	0.003	0.014	45.95	99.89
R2-4	0.27	30.05	20.09	0.41	2.87	0.01	0.81	0.01	0.011	0.14	45.34	99.88
N4-L3	0.22	30.62	20.42	0.2	2.7	0.059	0.24	0.01	0.007	0.013	45.48	99.81
N10-L1	0.32	30.82	19.39	0.08	1.99	0.05	0.49	0.01	0.003	0.013	46.78	99.9
N6-L2	0.15	30.09	20.15	0.33	4.66	0.002	0.84	0.01	0.002	0.012	43.66	99.89
N7-L3	1.52	29.46	18.48	0.58	5.24	0.086	0.59	0.16	0.015	0.031	43.76	99.9
N2-L1	0.31	26.33	21.26	0.37	9.85	0.004	0.39	0.01	0.001	0.013	41.37	99.89-
N10-L2	0.71	51.86	0.31	0.3	4.79	0.007	0.79	0.21	0.011	0.008	40.9	99.88
N10-L4	0.97	50.58	1.9	0.3	5.18	0.009	0.93	0.32	00.6	0.001	39.68	99.88
N4-L2	0.011	29.9	21.9	0.54	1.98	0.081	0.05	0.007	0.007	0.002	45.5	
N3	0.85	50.8	1.54	0.33	5.02	0.02	0.02	0.669	0.013	0.022	40.1	
N4	0.00	1.25	47.6	0.028	2.14	0.001	0.00	0.08	0.00	0.00	49.0	
N5	0.4	0.48	45.39	0.38	3.59	0.002	0.11	0.01	0.003	0.014	49.49	99.86
N7	0.00	11.6	11.7	0.25	57.1	0.023	0.01	0.001	0.018	0.00	19.2	
N8	0.56	27.1	23.6	0.944	6.5	0.085	0.05	0.002	0.015	0.019	41.1	

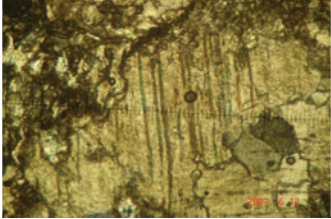R=Fariedah Belt   N 1-8 =Al-Thanyiah Belt   N10 = Tuba'a Al-Thanyiah samples
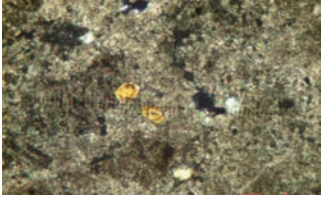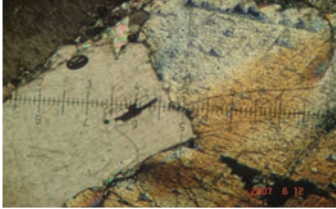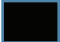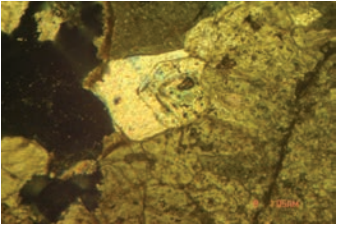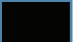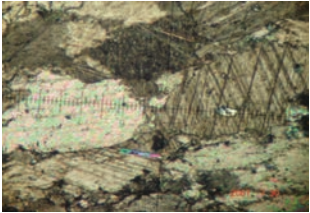
DIAGENETIC PHASE	EXPOSED TO SHALLOW BURIAL	INTERMEDIATE TO DEEP BURIAL	UPLIFT	TEXTURAL RELATIONSHIPS
DOLOMITIZATION	■■■■			
FRACTURE I		■■■		
STYLOLITE		■		
HYDROTHERMAL MAGNESITE		■■		
FRACTURE II		■		
BRECCIATION		■		
HYDROTHERMAL DOLOMITE		■		
LATE CALCITE			■	

Figure 5- Diagenetic sequence inferred for the Al-Thanyiah Group carbonates in the study area. Bars indicate the relative depths of different diagenetic events. The transition between shallow burial and intermediate-to-deep burial is interpreted as the onset of stylolitization; the transition from burial to uplift is defined by the initiation of the retrograde thermal history.

were metamorphosed. The fact that the sedimentary structures are preserved may indicate a dolomitization process in a not too advanced diagenetic stage. Dolomites seem to be the dominant carbonates within the Precambrian sedimentary record (Tucker and Wright, 1990; Melezhik et al., 2001; Prasannakumar et al., 2002; Melezhik and Fallick, 2003; Herrero et al., 2011).

The origins of these rocks have been widely disputed (Tucker, 1982), though there are data to suggest that in that time, the physical conditions (T and P_{CO_2}) and Mg^{2+}/Ca^{2+} ratios would promote dolomitization processes whereby preexisting calcite was replaced by dolomite.

In the upper Proterozoic and lower Paleozoic, the $\delta^{18}O$ signature of marine carbonate material was significantly lower than those deposited later on (Allan and Wiggins, 1993). D1 and D2 dolomite phases were probably formed at this time period, where low temperature dolomite acquired this low $\delta^{18}O$ signature during formation (Allan and Wiggins, 1993). These dolomites were later on totally recrystallized during burial and metamorphism and this might further lower the $\delta^{18}O$ values (Allan and Wiggins, 1993). The recrystallization is also confirmed by the coarser crystal size of dolomite and other components when it replaces either mud dominated carbonates or grain dominated carbonates. Later recrystallization of these dolomitic rocks during burial and subsequent metamorphism caused an increase in crystal size and homogenization of geochemical signatures (Sibley and Gregg, 1987; Morse and Mackenzie, 1990; Moore, 2001; Prasannakumar et al., 2002; Herrero et al., 2011).

The absence of stylolites affecting magnesite cf. M1-M4 and dolomite D1 and D2 is an indication of the burial and chemical compaction as well as intense tectonic activities in that these magnesites and dolomites subjected. Accordingly, this replacement event should represent burial and metamorphism stages or, as interpreted above, the resetting by recrystallization of initial geochemical signatures.

B. Genesis and Origin of The Magnesite Belt: The main requirements for magnesite formation through dolomite replacement include an increase in the Mg^{+2}/Ca^{+2} ratio and P_{CO_2}. Compaction, metamorphism

and ultra-basic rocks intrusion during burial of the Al-Thanyiah Group affected siliciclastic deposits, specifically shales, which supplied water enriched in Mg^{2+}, as well as hydrothermal solutions rich in Mg^{+2} comes from ultra-basic intrusions.

In addition, during diagenesis, fluids enriched in Mg^{+2} may have been formed by Mg-liberating reactions resultant of the formation of chloritization (Morteani et al., 1982; Lugli et al., 2002). This water increased the Mg^{+2}/Ca^{+2} ratio and contributed to magnesite precipitation (Möller, 1989). Experimental work (Franz, 1989) suggests that the stability field of magnesite ranges from very low temperatures and pressures (sedimentary environment) to extremely high temperature conditions (upper mantle). A higher temperature shifts the mineral stability from the dolomite stability field to the magnesite field (Johannes, 1970; Kralik et al., 1989; Prasannakumar et al., 2002 Herrero et al., 2011). Hence, processes such as Mg^{+2} enriched hydrothermal fluid circulations could both enhance Mg^{+2}/Ca^{+2} ratios in fluids and contribute to increase temperature conditions (Siegl, 1984; Herrero et al., 2011). Magnesite appears in outcrop replacing both the dolomite and the dolomitic limestone rocks. The replacement front is appreciable in the field and the textural relationship of the magnesite to fractures, fault planes, large cavities and vugs and bedding planes reveals that the hydrothermal fluids used them as conduits to pass through the rocks (Lugli et al., 2000). The extent and distribution of replacement was controlled by the location of fractures, the nature of the precursor rock and the permeability and the capacity of the solution to pass through (Smith and Davies, 2006).

Magnesite formation is possible at both low and high contents of CO_2 in the fluid phase (Möller, 1989). However, an increase in CO_2 pressure favors the precipitation of magnesite (Möller, 1989) at moderate temperatures. Hydrothermal fluids would increase the CO_2 pressure, similarly to the increase of CO_2 volume produced by metamorphism of calcareous sequences by emplacement of igneous intrusions (Morad, 1998).

The formation of magnesite with iron rich rims (M2), has been explained by Johannes (1970) to be due to retrograde metamorphism. In M2, the decrease in Fe and Mn as the Mg content increases is the outcome

of iron and manganese being usually incorporated into the solid phase, whereas magnesium, strontium and barium are preferentially left in the fluid. This leads to a distinct zoning of magnesite, with more Fe-poor cores and Fe-rich rims as temperature decreases (Johannes, 1970). As magnesite precipitates, residual fluids are enriched in calcium.

According to the field observations and petrographic examination of the magnesite-bearing horizons, the magnesite formation took place during hydrothermal fluid circulation events derived from the ultra-basic intrusions associated with intense tectonic events. It could also be modified in response to water–rock interactions or by contributions of oxidized carbon with meteoric waters (Souza et al., 1995).

The studied rocks have undergone several diagenetic processes associated with metamorphic alteration events e.g. thermal metamorphism by intrusion of ultra-basic magma, rather than resulting from interactions with later post-depositional diagenetic fluids.

Magnesites are most probably interpreted as a result of heating up the circulating and related formational and diagenetic fluids, which have reacted with the original dolomites and metamorphic rocks, and probably associated with meteoric waters and/or reactions with underlying basement rocks e.g. schist and granitic rocks (Veizer, 1989).

Magnesite appears to have formed subsequently to stylolitization of the first dolomite rocks (D1 and D2). At least 500 m of burial is required for stylolite formation in limestones (Fabricius, 2000). Brecciation and boxwork vugs structures (which is observed in the field) are attributed to hydro-fracturing (Davies, 2004; Smith and Davies, 2006) produced when the fluids were expulsed along high permeability faults and fractures into the surrounding strata. The fluids were injected into the sequence, causing brecciation and fracturing of the host rock by pressure release (Prasannakumar et al., 2002; Smith and Davies, 2006; Herrero et al., 2011).
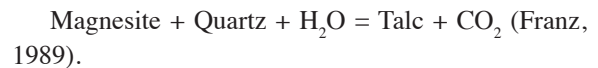
When the pore size is large enough to be appreciable at outcrop scale e.g. as it is observed in the field, it is observed that they appear aligned to faults and bedding planes and in close relation to the magnesite formation front. Therefore, dolomite

is interpreted to have been formed postdating the magnesitization event, and that the dolomitizing fluids entered though the rocks using similar pathways, where dolomite formed due to magnesite replacement caused by interaction with hydrothermal fluids (Lugli et al., 2000; Kilias et al., 2006). It is most probably suggested that both dolomite and magnesite rocks are formed under the influence of the same evolving hydrothermal fluids comes from ultra-basic intrusions.

Talc appears in the boundaries between the crystals of magnesite and dolomite and in joints, fractures and stylolites within the magnesite and later dolomite phases. The reaction assumed for the main stage of talc mineralization within dolomite rocks is:

3Dolomite + 4Quartz + H_2O = Talc + 3cal + 3CO_2 (Franz, 1989).
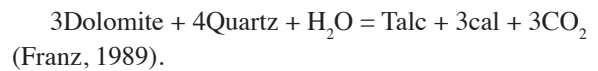
The reaction of talc formation from magnesite is:

Magnesite + Quartz + H_2O = Talc + CO_2 (Franz, 1989).

The latter reaction may even occur at low temperatures (Winkler, 1988). Bucher and Frey (1994) described the formation of talc through decarbonation reactions of magnesite at temperatures lower than 500 °C and from fluids of low P_{CO2}.

The formation of talc from dolomites occurs at temperatures between 300 °C and 400 °C. Therefore, the presence of talc related to D1 and D2 implies that these dolomites underwent temperatures as high as 400 to 500 °C.

The presence of forsterite associated to the magnesite provides additional clues to interpret the interaction of the studied rocks with hydrothermal fluids. Experimental work has shown that by rising total fluid pressure and P_{CO2}, and decreasing temperature, forsterite can form through the reaction of talc and magnesite (Franz, 1989).

Talc + Magnesite = ¼ Forsterite + CO_2 + H_2O … at almost 400-500[0]C associated with high compressional pressure

Dolomite and talc probably formed under the influence of hydrothermal fluid, and the later should be cooling of this fluid and varying chemical composition led to the formation of forsterite.

The brucite appears in the fractures, boundaries between magnesite crystals or embedded in the magnesite crystals. The brucite is most probably formed by hydration of magnesite mineral during diagenetic phases (Keer, 1975).

C. Late Calcite Cement: Calcite appears as a late diagenetic phase filling intracrystalline pores, displaying consistent Fe zoning. This Low-Mg calcite suggests that the rocks were exhumed and subjected to surficial diagenetic processes (Moore, 2001). This idea confirms the inferred oxidation conditions in a meteoric surface environment interpreted for the increase in Fe^{+2} contents (Pierson, 1981). This late diagenetic calcite reduces porosity and permeability in outcrop.

9. Conclusion

The detailed analysis of the magnesite and dolomite phases in newly introduced Al-Thanyiah Group permits to constrain the model of formation and conditions that accounted for their development. Detailed sedimentological, petrographic and geochemical analyses of the magnesite-carbonate rocks that most probably belong to Neoproterozoic-Ediacaran (?) succession reveals a complex paragenetic evolution. The studied area located 360 km east of Sana'a City and 130 km east of Ma'rib city.

Based on facies association analyses and their vertical and lateral stacking pattern, the sequence is interpreted as a mixed siliciclastic-carbonate platform. The age of the succession suggested as Ediacaran based on the regional stratigraphic correlation with the Oman and Ethiopia, where there are no any fossils content observed. These rocks have suffered from intense metamorphism and associated transformations. Magnesite, dolomite and minor traces of talc, brucite and very rare forsterite together with geochemical data and outcrop observations reveal that the principal processes that affected these rocks were related to burial diagenesis, ultrabasic intrusions e.g. peridotite and hornblendite. and associated up heated diagenetic fluids circulation. Two early dolomite phases (D1 and D2) appear as crystalline replacive dolomite, which formed through dolomitization of the original peritidal limestones under evaporative conditions. Crystal sizes variations between D1 and D2 depend on the texture of the precursor limestone. The recrystallization of these dolomites took place during burial. Cross-checking

the field observations together with petrographic examinations indicate that the magnesite (M1, M2 and M3) were formed through the replacement of D1 and D2 by Mg^{+2} enriched fluids that entered the system via stylolite, vugs, faults, fractures and bedding planes. The enriched Mg^{+2} in the fluids were probably sourced by compaction of lateral detrital sediments and the transformation of clays into chlorites. These are basically associated with intense tectonism and metamorphism.

In addition, possible Mg^{+2} enriched up heated fluids e.g. heat comes from introduced ultrabasic rocks, may have contributed to increase the Mg^{+2}/Ca^{+2} ratio and temperature. The absence of zoning of the magnesite phases into an initial iron-poor phase reflects variations towards lower temperature conditions. Talc, brucite, forsterite and the late dolomites formed in relation to hydrothermal fluids. Talc associated with dolomite could have formed through de-carbonation of magnesite at temperatures lower than 500 °C. Forsterite formed through the reaction of talc and magnesite, probably as the fluids cooled down probably at temperature more than 500 ^{0}C.

A late diagenetic calcite phase appears in some samples replacing magnesite and dolomite phases. This low-Mg calcite was precipitated during telo-diagenesis, when the rocks interacted with surficial fluids of meteoric origin.

Although some questions such as the precise temperature and the mechanisms of circulation of the up heated fluids remain unclear, our study reveals that the occurrence of magnesite deposits within the Al-Thanyiah Group is the result of complex diagenetic and heated processes associated with intense tectonism and metamorphism e.g. compressional pressure. Both the prior dolomites and the presence of siliciclastic beds suggest an important role for these deposits in the formation of magnesitization fluids. The textural characterization both in the field and in thin section analysis of the magnesite and dolomite as well as their geochemical signatures permits to develop a model of their origin and mechanism of formation that supports the hydrothermal origin of spary magnesite by replacement of precursor dolomites, similarly to those described in other magnesite deposits like those of the Eugui or Rubian deposits in Spain (Lugli et al., 2000; Kilias et al., 2006).

References

Allan, J.R., Wiggins, W.D. 1993. Dolomite reservoirs; geochemical techniques for evaluating origin and distribution: American Association of Petroleum Geologists Continuing Education Course Note Series 36, 129p.

Al-Mashaikie, S. Z. 2006. Preliminary Report; Petrography and geochemistry of Al-Thanyiah magnesite-carbonate belt in Ma'rib District, NW Yemen. Geological Survey and Mineral Resource Board, Ministry of Oil, Sana'a, Yemen, 34p.

Al-Mashaikie, S. Z. 2007. Petrography, geochemistry and technical report of the Carbonate - Magnesite rocks belt in Al-Thanyiah region NE YEMEN, Unpublished Geological Research. Geological Survey and Mineral Resource Board, Ministry of Oil, Sana'a, Yemen, 82p.

Al-Mashaikie, S. Z. 2008. Geochemistry, mineralogy and industrial evaluation of the first discover of Magnesite – Carbonate belt rocks, in Yemen. 8th conference of Mineral resources in the Arabian Countries, Amman, Jordan, 32p.

Beydoun, Z.R., As-Sururi, M., El-Nakhal, H., Al-Ganad, I., Baraba, R., Nani, A., Al-Awah, M. 1998. International Lexicon of stratigraphy, vol., Asia, Fascicule 3(10b2), Republic of Yemen. IUGS publication No. 34, 245p. Sedimentary cover. Z.geol. Wiss., 26(5/6) 517-529 Berlin.

Brasier, D. Martin, Allen, A Phillip, Leather, J. 2011. Chapter 20, The Abu Mahara Group (Ghubrah and Fiq formations), Jabal Akhdar, Oman. Geological Society, London, Memoirs 36, 251-262.

Bucher, M., Frey, M. 1994. Petrogenesis of Metamorphic Rocks. Springer-Verlag, 318p.

Davies, G.R. 2004. Hydrothermal (thermobaric) dolomitization: rock fabric and organic petrology support for emplacement under conditions of thermal transients, shear stress, high pore fluid pressure with abrupt pressure transients, hydrofracturing, episodic rapid fluid flow, and instantaneous cementation by saddle dolomite. In: Davies, G.R., Packard, J., McAuley, R. (Ed.), Dolomite Seminar and Core Conference. Canadian Society of Petroleum Geologists, Calgary, 20p.

Dragastan, O.N., Richter, D.K. 2011. Stromatolite and calcareous algae of Munder Formation (Tithonian- -Berriasian) From NW Germany. Acta Palaeontologica Romaniae 7, 139-168.

Dulski, P., Morteany, G. 1989. Magnesite formation by CO2 metasomatism during regional metamorphism of the ultrabasic rocks of the Ochsner serpentinite (Zillertaler Alpen, Tyrol, Austria). Monograph Series on Mineral deposits, 28. Borntraeger, Berlin-Stuttgart, 95–104.

Fabricius, I.L. 2000. Interpretation of burial history and rebound from loading experiments and occurrence of microstylolites in mixed sediments of Caribbean sites 999 and 1001. In: Leckie, R.M., Sigurdsson, H., Acton, G.D., Draper, G. (Ed.), Proceedings of the Ocean Drilling Program, scientific results 165: College Station, Texas, Ocean Drilling Program, 177–190.

Franz, G. 1989. Stability of magnesite in carbonate–silicate assemblages; a review. Monograph Series on Mineral deposits, 28. Borntraeger, Berlin-Stuttgart, 259–268.

Geomine Company 1984-1985. Preliminary Report; Industrail rocks and minerals in Ma'rib District. Unpublished report, Geological Survey and Mineral Resources Board, Romaine, 210p.

Herrero, M.J., Martín-Pérez, A., Ana M. Alonso-Zarza, Gil-Peña, I., Meléndez, A., Martín-García, R. 2011. Petrography and geochemistry of the magnesites and dolostones of the Ediacaran Ibor Group (635 to 542 Ma), Western Spain: Evidences of their hydrothermal origin. Sedimentary Geology 240, 71-84.

IUGS, 2009. International Stratigraphic Chart. International Commision on Stratigraphy. http://www. stratigraphy.org/2009.

Johannes, W. 1970. Zur entstehung von magnesitvorkommen. Neues Jahrbuch für Mineralogie Abhandlungen 113, 274–325.

Kralik, M., Aharon, P., Schroll, E., Zachmann, D. 1989. Carbon and oxygen isotope systematics of magnesites: a review. In: Moller, P. (Ed.). Magnesite, Monograph Series on Mineral deposits, 28. Berlin-Stuttgart, Borntraeger, 197–224.

Kilias, S.P., Pozo, M., Bustillo, M., Stamatakis, M.G., Calvo, J.P. 2006. Origin of the Rubian carbonate-hosted magnesite deposit, Galicia, NW Spain: mineralogical, REE, fluid inclusion and isotope evidence. Mineralium Deposita 41, 713–733.

Lugli, S., Torres–Ruiz, J., Garuti, G., Olmedo, F. 2000. Petrography and geochemistry of the Eugui magnesite deposit (Western Pyrenees, Spain): evidence for the development of a peculiar zebra banding by dolomite replacement. Economic Geology 95, 1775–1791.

Lugli, S., Morteani, G., Blamart, D. 2002. Petrographic, REE, fluid inclusion and stable isotope study of magnesite from the Upper Triassic Burano Evaporites (Secchia Valley, northern Apennines): contributions from sedimentary, hydrothermal and metasomatic sources. Mineral Deposits 37, 480–494.

Machel, H.G., Lonnee, J. 2002. Hydrothermal dolomite; a product of poor definition and imagination. Sedimentary Geology 152, 163–171.

Melezhik, V.A., Fallick, A.E., Medvedev, P.V., Makarikhin, V.V. 2001. Palaeoproterozoic magnesite: lithological and isotopic evidence for playa/sabkha environments. Sedimentology 48, 379–397.

Melezhik, V.A., Fallick, A.E. 2003. δ^{13}C and δ^{18}O variations in primary and secondary carbonate phases: several contrasting examples from Palaeoproterozoic 13C–rich dolostones. Chemical Geology 201, 213–228.

Meister, P., Judith A. Mckenzie, J., Bernascon, S. M., Brack, P. 2013 Dolomite formation in the shallow seas of the Alpine Triassic. Sedimentology 60, 270–291.

Morse, J.V., Mackenzie, F.T. 1990. Geochemistry of sedimentary carbonates. Developments in Sedimentology, 48. Elsevier Scientific Publication Co, New York, 696p.

Moore, C.H. 2001. Carbonate reservoirs: porosity evolution and diagenesis in a sequence stratigraphic framework. Developments in Sedimentology 55, 444.

Morad, S. 1998. Carbonate cementation in sandstones: distribution patterns and geochemical evolution. In: Morad, S. (Ed.). Carbonate Cementation in Sandstones: Distribution Patterns and Geochemical Evolution: International Association of Sedimentologists Special Publication 26, 1–26.

Morteani, G., Möller, P., Schley, F. 1982. The rare earth element contents and the origin of the sparry magnesite mineralizations of Tux-Lanersbach, Entachen Alm, Spiessnägel, and Hochfilzen, Austria, and the lacustrine magnesite deposits of Aiani-Kozani, Greece, and Bela Stena, Yugoslavia. Economic Geology 77, 617–631.

Möller, P. 1989. Minor and trace elements in magnesite. In: Moller, P. (Ed.). Magnesite, Monograph Series on Mineral deposits, 28. Berlin–Stuttgart, Borntraeger, 173–196.

Müller, G., Irion, G., Förstner, U. 1972. Formation and diagenesis of inorganic Ca–Mg carbonates in the lacustrine environment. Naturwissenschaften 59, 158–164.

Nash, M. C., Troitzsch, U., Opdyke, B. N., Trafford, J. M., Russell, B. D., Kline, D. I. 2011. First discovery of dolomite and magnesite in living coralline algae and its geobiological implications. Biogeosciences 8, 3331–3340.

Prasannakumar, V., Vikas, C., Kumar, S.N. 2002. Constraints on the origin of south indian magnesite deposits. Boletim Paranaense de Geociências 50, 15-20.

Perri, E., Manzo, E., Maurice E., Tucker, M. E. 2012. Multi-scale study of the role of the biofilm in the formation of minerals and fabrics in calcareous tufa. Sedimentary Geology 263-264, 16–29.

Pierson, J. 1981. The control of cathodoluminescence in dolomite by iron and manganese. Sedimentology 28, 601–610.

Pohl, W. 1989. Comparative geology of magnesite deposits and occurrences. In: Moller, P. (Ed.). Magnesite, Monograph Series on Mineral deposits, 28. Berlin-Stuttgart, Borntraeger, 1–14.

Pohl, W. 1990. Genesis of magnesite deposits — models and trends. Geologische Rundchau 79, 291–299.

Pueyo, J.J., Inglés, M. 1987. Magnesite formation in recent playa lakes, Los Monegros, Spain. In: Marshall, J.D. (Ed.). Diagenesis of Sedimentary Sequences, Geological Society Special Publication, 119–122.

Quemeneur, J.M. 1974. Les gisement de magnesite du Pays Basque: Cadre geoligique et sedimentologique; genese de la magnesite en milieu sédimentaire. Diss. Univ. Paris VI, (unpublished), 210p.

Schroll, E. 2002. Genesis of magnesite deposits in the view of isotope geochemistry. Boletim Paranaense de Geociências, UFPR 50, 59–68.

Sibley, D.F., Gregg, J.M. 1987. Classification of dolomite rock textures. Journal of Sedimentary Petrology 57, 967–975.

Siegl, W. 1984. Reflections on the origin of sparrymagnesite deposits. In:Wauschkuhn, A., Kluth, C., Zimmermann, R.A. (Eds.), Syngenesis and Epigenesis in the Formation of Mineral Deposits. Springer-Verlag, Berlin, 177–182.

Smith, L.B., Davies, G.R. 2006. Structurally controlled hydrothermal alteration of carbonate reservoirs: introduction. American Association of Petroleum Geologists Bulletin 90, 1635–1640.

Souza, R.S., De Ros, L.F., Morad, S. 1995. Dolomite diagenesis and porosity preservation in lithic reservoirs, Carmópolis Member, Sergipe–Alagoas Basin, Northeastern Brazil. American Association of Petroleum Geologists Bulletin 79, 725–748.

Spadafora, A., Perri, E., Judith, A., Mckenzie, J.A, Vasconcelos, C. G. 2010. Microbial biomineralization processes forming modern Ca:Mg carbonate stromatolites. Sedimentology 57, 27–40.

Teedumäe, A., Shogenova, A., Kallaste, T. 2006. Dolomitization and sedimentary cyclicity of the Ordovician, Silurian, and Devonian rocks in South Estonia. Proceedings of the Estonian Academy of Sciences, Geology 55 (1), 67-87

Tucker, M.E. 1982. Precambrian dolomites: petrography and isotopic evidence that they differ from Phanerozoic dolomites. Geology 10, 7–12.

Tucker, M.E. 1988. Technique in Sedimentology. Blackwell scientific publication: 394 p.

Tucker, M.E., Wright, P. 1990. Carbonate Sedimentology. Blackwell Scientific Publications, London, 482p.

Veizer, J. 1989. Strontium isotopes in seawater through time. Annual Review of Earth and Planetary Science 17, 141–167.

Wacey, D., Wright, D.T., Boyce, A.J. 2007. A stable isotope study of microbial dolomite formation in the Coorong Region, South Australia. Chemical Geology 244 155–174

Winkler, H.G.F. 1988. Petrogenesis of Metamorphic Rocks. Narosa Publishing House, New Delhi, 348p.

Zachmann, D.W. 1989. Mg-carbonate deposits in freshwater environment. In: Moller, P. (Ed.). Magnesite, Monograph Series on Mineral Deposits, 28. Berlin-Stuttgart, Borntraeger, 61–94.

Zachmann, D.W., Johannes, W. 1989. Cryptocrystalline magnesite. In: Moller, P. (Ed.). Magnesite, Monograph Series on Mineral Deposits, 28. Berlin-Stuttgart, Borntraeger, 15–28.

PLATES

PLATE I-   Field photographs show the Al-Thanyiah major belt and the stratigraphic units in the Al-Thanyiah area.

Figure 1- General view of the Al-Thanyiah Mountain Belt.

Figure 2- The middle Fariedah Mountain which is situated in the southern part of the Al-Thanyiah Belt, shows the major productive Unit-A of magnesite rocks.

Figure 3- The northern Fariedah Mountain which is situated in southern part of the Al-Thanyiah Belt and shows the stratigraphic Units of A, B and C.

Figure 4- General view shows Fariedah Al-Thanyiah Mountain belts.

Figure 5- General view shows Tuba'a Al-Thanyiah, which is situated in the northern part of the Al-Thanyiah Belt.

Figure 6- General view of the Al-Thanyiah major belt shows the major stratigraphic unit (A, B and C).

Figure 7- Stratigraphic Unit D, E and F which is identified in the major the Al-Thanyiah Mountain.

Figure 8- Stratigraphic Unit E and F which is identified in the major the Al-Thanyiah Mountain.
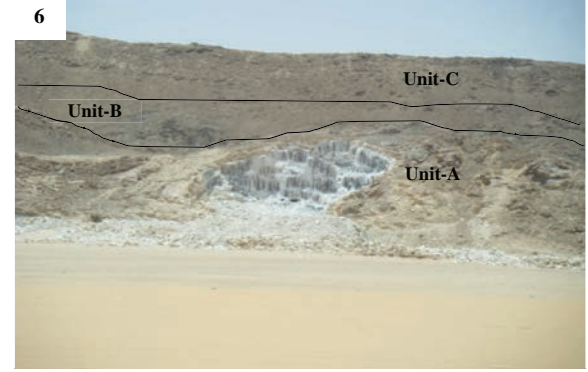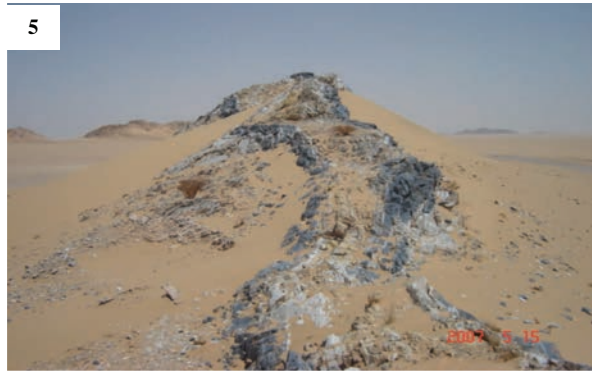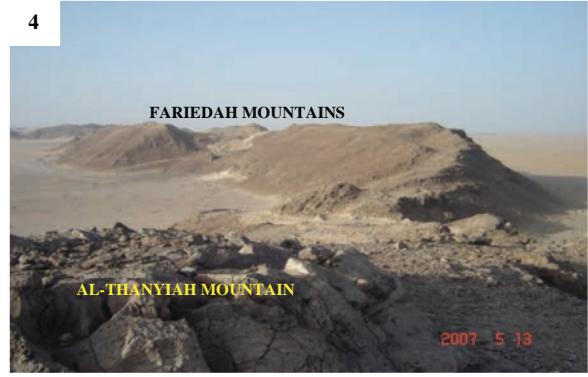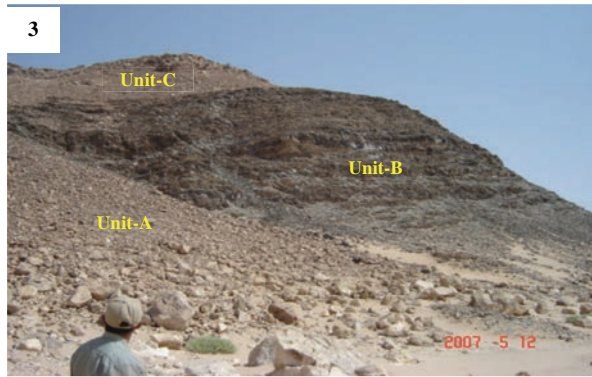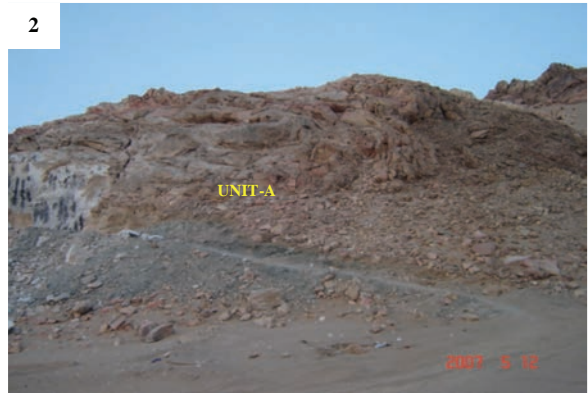
PLATE I
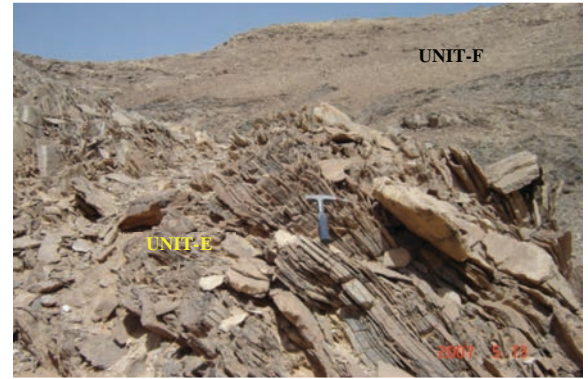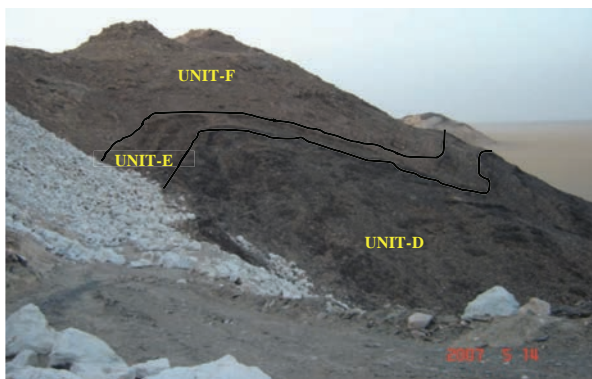
PLATE II- Field photographs show the Al-Thanyiah major belt and the stratigraphic units in Al-Thanyiah area.

Figure 1- Very large crystal of magnesite, which was recognized in the Al-Thanyiah Major Belt.

Figure 2- Hydrothermal solution effect shows in the Tuba'a Al-Thanyiah Belt in the northern limit,

Figure 3- Black magnesite rocks which was recognized at the top of the Al-Thanyiah Major Belt.

Figure 4- Red magnesite rocks which was recognized at the bottom of the Al-Thanyiah Major Belt.

Figure 5- Talc-schist rocks which was recognized at the top of the Al-Thanyiah Major Belt.

Figure 6- Talc-schist and magnesite rocks which were recognized at the top of the Al-Thanyiah Major Belt. Note the effect of intense folding and trusting in the rock successions.

Figure 7- Dolomite-marble rocks which was recognized in the northern limit of the Tuba'a Al- Thanyiah Belt.

Figure 8- Large ultra-basic igneous intrusion, which was recognized intersecting the Jabal Al-Quroon Mountain in front of Major the Al-Thanyiah Belt.
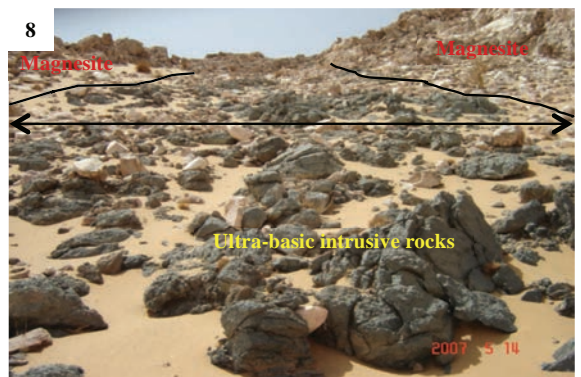
PLATE II

PLATE III- Photomicrographs show the mineralogical constituents and the textures of magnesite in Al-Thanyiah Belt. (Mg) magnesite, (Dl) dolomite. (Br) brucite, and (Tl) talc.

Figure 1- Phenocrysts of magnesite with undulose extinction form the main magnesite-bearing horizon (CNx40X).

Figure 2- Euhedral magnesite crystals with undulose extinction (CNx40X).

Figure 3- Subhedral magnesite crystals with undulose extinction (CNx40X).

Figure 4- Anhedral magnesite crystals with undulose extinction. Note the brucite crystal in lower left of the photo (CNx40X).

Figure 5- Porphyritic texture of magnesite phenocrysts surrounded with small crystals. Note the green flakes of talc crystals (CNx40X).

Figure 6- Flakes of green talc embedded within magnesite crystals (CNx40X).

PLATE III